Congresso ABRISCO 2017

A Computational Fluid Dynamic Code Based on Collision Algorithm and Flamelet Combustion Model for Advanced Explosion Simulation

Tatiele Dalfior Ferreira, Sávio Souza Venâncio Vianna
University of Campinas

INTRODUCTION

Accidentals involving gas explosion is a concern on different industrial plants, especially when large quantities of flammable gas are involved such as the petroleum industry. The analysis of gas explosion is an important step of the risk analysis to ensure the safety of installations where an explosion can occur. The gas explosion hazard assessment can be very helpful to improve the design of the existing or new installations and characterize the extent of the hazard.

Making realistic predictions of the effects of an accidental explosion is a difficult task due to the complexity of the physical and chemical processes involved. There are limitations to experimental data available and full-scale experimental tests is often impracticable or prohibitively expensive [1]. Thus, theoretical modelling and simulation have been employed to assess gas explosion hazards.

The correctly modelling of large-scale explosion involves the relevant parameters such as geometrical design and physical effects. The numerical simulation using Computational Fluid Dynamics (CFD) takes into account the geometries found in industrial plants. It is considered the best available approach when modelling gas explosion. The representation of all geometric scales is possible, but infeasible, by using CFD techniques. It requires a very fine mesh resolution and extensive computational effort and costs. Unstructured meshes and adaptative mesh refinement have been used [2,3] in order to reduce the geometrical approximations, but the approach is still computationally quite expensive and it needs to be improved.

The Porosity/Distributed Resistance (PDR) have been applied to model the geometry in CFD simulations and thus assess a great level of geometrical details. By using this method the large-scale geometry is fully represented and resolved, while the small-scale objects are taken together locally and approximated in terms of their effective porosity and resistance to the flow [11]. The PDR modelling is widely used for numerical simulations of gas explosion and has been successful within the constraints of its modelling approximations [4,5].

This paper presents a finite-volume code that uses the PDR concepts to represent the geometry for the fluid flow and explosion analysis. Simulations of cold flow and preliminary results for explosion simulation are presented and discussed in the results section.

The PDR (Porosity Distributed Resistance) Approach

By following the Porosity Distributed Resistance approach the small obstacles that are not solved by the computational mesh occupy part of the computational cell so that only part of the control volume is available to the flow. Figure 1 shows a typical control volume partially occupied by a small object.

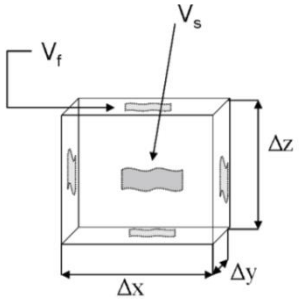

Figure 1 - Computational cell partially occupied by a solid object [6]. δx, δy and δz represents the dimensions of the computational cell. V_s represents the volume occupied by the solid obstacle and V_f represents the volume available to the flow.

Considering the control volume shown above, the porosity volume fraction can be defined as:

$$\beta_V = \frac{V_f}{V_f + V_s} = \frac{V_f}{\delta x \delta y \delta z}$$

In the same way, the area porosity can be defined on each one of the three directions (x, y and z). In x direction, the porosity area can be expressed as:

$$\beta_x = \frac{\int_{surface} dydz}{\delta y \delta z}$$

The porosity values for the area and volume are modified according to the blockage of the computational cell. The values ranging from 0.0 (when the cell is fully blocked) to 1.0 (when the computational cell is completely open).

The PDR methodology also considers that the unresolved objects (that forms a porous mesh) offer additional resistance to the flow and are responsible for increasing the production of turbulence. As consequence, the transport governing equations are modified.

Considering the control volume shown in figure 1, the application of the conservation laws give the following modified equations for mass (3) and momentum (4):

$$\frac{\partial}{\partial t}(\beta_v \rho) + \frac{\partial}{\partial x_i}(\beta_i \rho U_i) = 0$$

$$\frac{\partial}{\partial t}(\beta_v \rho U_i) + \frac{\partial}{\partial x_j}(\beta_j \rho U_j U_i) = -\beta_v \frac{\partial p}{\partial x_i} + \frac{\partial}{\partial x_j}(\beta_j \sigma_{ij}) + \beta_v \rho g_i + R_i$$

Here, U_i is the velocity component in the x_i direction; ρ is the density; p is the pressure; g_i is the gravitational acceleration; σ_{ij} is the turbulent flux of momentum and R_i s the additional resistance caused by the obstacles [5-6].

METHODOLOGY

The developed code comprises two main steps. In the first one a grid is created and the geometry under study is described as porous media based on the Gilbert-Johnson-Keerthi (GJK) distance algorithm. In the second step the solver's code solves the equations that describe the fluid flow for each computational cell based on the volume and area porosity obtained in the previous step. The code was named PFS (Porosity Flow Solver) and has been developed at the University of Campinas. All post processing is conducted in an open source tool "Kitware Paraview".

Creating the Computational Mesh

In order to generate a computational mesh, initially, a structured Cartesian grid is considered as show in Figure 2. The Gilbert-Johnson-Keerthi (GJK) distance algorithm is applied to calculate the porosity values for each computational cell.

The use of the GJK approach to obtain area and volume porosity was introduced by Moreira et.al [7]. By using this methodology it is possible to check the collision between a cell of the computational grid and each solid object of the geometry under study. As result, each cell is addressed with porosity volume and area porosity for each one of its faces. The GJK algorithm was validate for different object shapes. It has been proved able to obtain porosity values for simple and complex geometries.

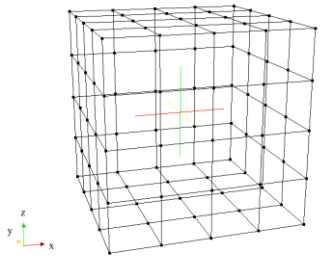

Figure 2 - Example of a structured Cartesian divided in uniform hexahedral cells.

The solver

The solver part of the code uses the computational grid and porosity values obtained in the previous step to solve the equations of the fluid flow. These equations comprises the mass, momentum and energy conservation. The standard k-epsilon model is used in the turbulence model. Initial parameters as fluid properties, operation conditions (pressure, temperature), Courant number, maximum residual and number of iterations are given by the solver operator.

The solver was built based on an explicit method. The governing equations are discretized by the central differencing scheme and integrated in the control volume using the finite volume methodology. The classical fourth order Runge-Kutta time marching approach is considered. Isentropic equations are also considered in order to couple the density and pressure variables.

Different boundary conditions are imposed. At inflow total pressure and total temperature is considered. At the outflow the static pressure is considered constant while the other variables are extrapolated from the interior. No flux is considered across the walls.

The maximum and average residual obtained by the calculations in a time step and in a previous time step is the main convergence criterion. The maximum number of iterations can also be used to stop the simulation.

RESULTS

Case studies of external flow by using a porous mesh to model the geometry under study is discussed here. Three cases were chosen for the analysis of cold flow: the flow around a rectangular cylinder and the flow over a step.

Flow around a rectangular cylinder

The study of flow around bluff bodies such as spheres, circular or rectangular cylinders comprises an important analysis for practical engineering application.

In order to evaluate the PFS code to describe fluid flow around bluff bodies, a squared box with length of 10 mm in each direction (z, y and z) was used as geometry under study and a gas flow was considered. Therefore a turbulent flow at Reynolds number equal to 22,000 was simulated. This value of Reynolds number is similar to that considered in previous study of experimental observations [9] and numerical simulation [10] of flow around a rectangular cylinder.

In a first step, the pre-processing tool was used to build a computational domain and calculate the porosity values. The domain comprised a rectangular box with 22cm in x direction and 8mm in y and z directions. The squared box was placed into the computational domain by considering the distance of 3.5 mm from y and z direction and 3 cm from x direction. The hexahedral cells with 1 mm of length was considered.

The squared box used in this study and the computational domain can be visualized in Figure 3a. Figure 3b shows the porosity values calculated for each computational cell based on the location of the box in the computational domain.

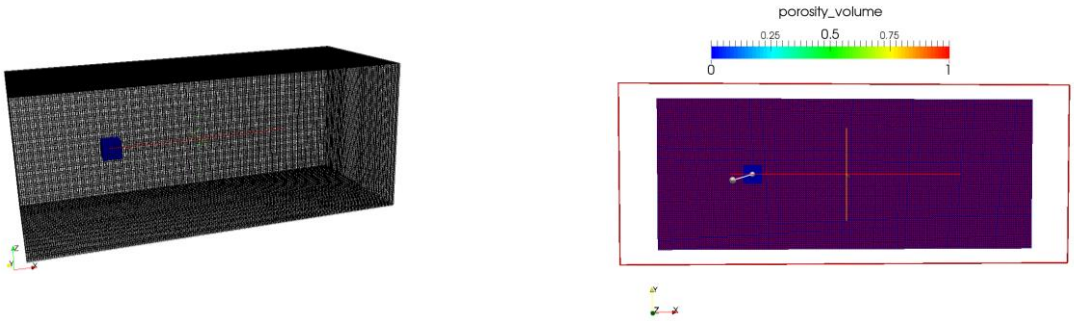

(a) (b)

Figure 3 - Computational domain used in the study of a flow around a rectangular cylinder. (a) Uniform hexahedral cells of the computational domain. (b) Porosity values calculated for all computational domain.

Based on the PDR methodology, it is possible to verify in Figure 3b that region of the computational domain that presents porosity values equal to 1 (red region), comprises the region of flow free while the region with porosity values equal to 0 (dark blue region), there will be no flow (the flow will be totally blocked by the box). The boundary cells of the squared box present different intermediated porosity values (green region), which indicates that such region will gives a resistance to the fluid flow (the flow will be partially blocked).

In the second step, a fluid flow was simulated by considering the computational domain and porosity values obtained in the previous step. A flow with Reynolds number of 22 000 was considered.

The boundary conditions were set so that the flow entrance in the computational domain was considered at the left boundary x, and the outlet boundary condition, with pressure gradient equal to zero, was considered at the right boundary x. The other borders of the computational domain were considered as wall where zero normal fluxes of mass, momentum and energy are imposed.

Figure 4 shows the result of the simulation. It is possible to observe that the velocity profile is similar to what is expected according to the literature and given by simulations using CFD commercial codes. The velocity increases in the side of the box parallel to the flow.

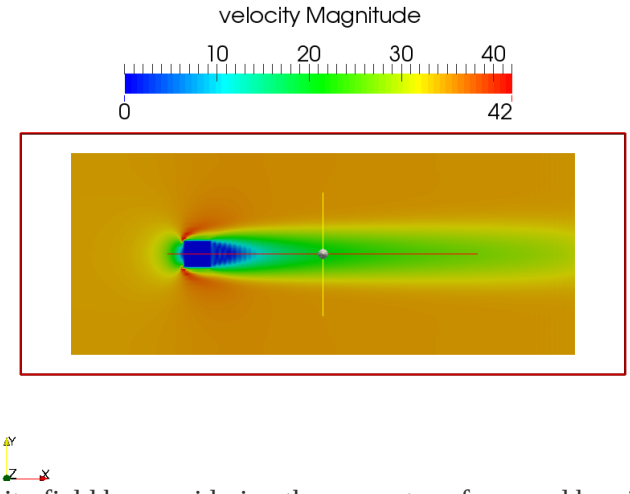

Figure 4 - Velocity field by considering the geometry of squared box in a porous mesh.

By considering the PDR model, it is possible to observe in figure 6 that the computational domain region set with porosity values equal to zero presents no velocity (dark blue square in figure 6), which indicates that there is no flow in such region.

Figure 5 presents the comparison between the simulation using the present code and the experimental data for a same flow [9]. It is possible to observe that the velocity profile in the centerline of the squared cylinder is similar to the experimental data. Concerning the turbulence, the results provided by the present code over predicts the turbulence intensity.

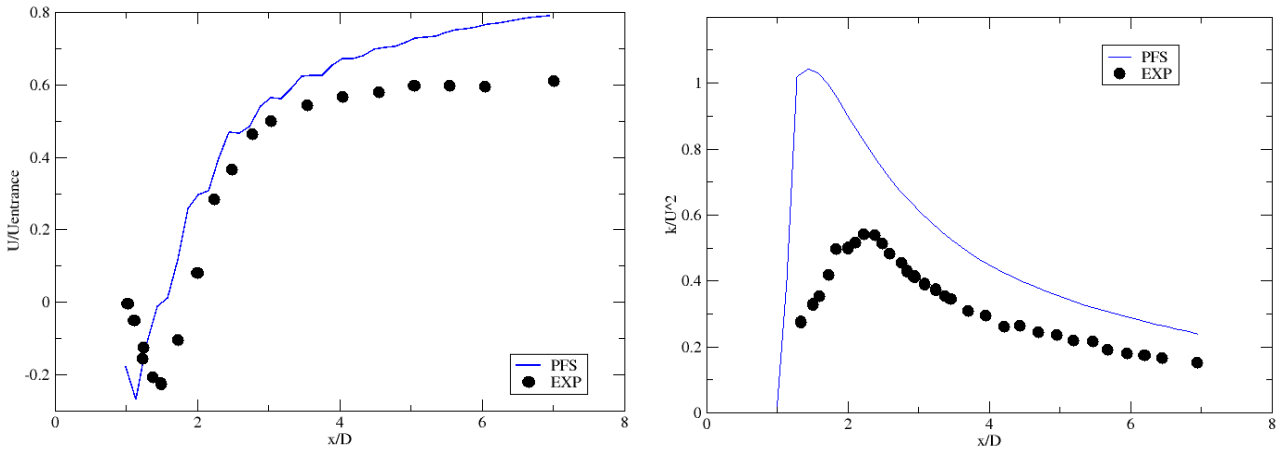

(a) (b)

Figure 5 – Results of the simulation of a turbulent flow over a rectangular cylinder. (a) Non-dimensional mean velocity along the centerline of the square cylinder and (b) the turbulence intensity.

Flow over a step

In this part of the study, a turbulent flow over a step were considered. A fluid flow at Reynolds number equal to 44,000 was simulated over a step with 0.01m of height and 0.04m of length. This value of Reynolds number is similar to that considered in previous study of numerical simulation [8] of turbulent flow over a step.

The computational domain, in this case, comprises a rectangular box with 0.34m in x direction and 0.03m in z direction e 0.01m in y direction. The step was placed ate the entrance of the computational domain and computational cells with 0.001m of length were considered.

The step geometry used in this study and the computational domain can be visualized in Figure 6 that shows the porosity values calculated for each computational cell.

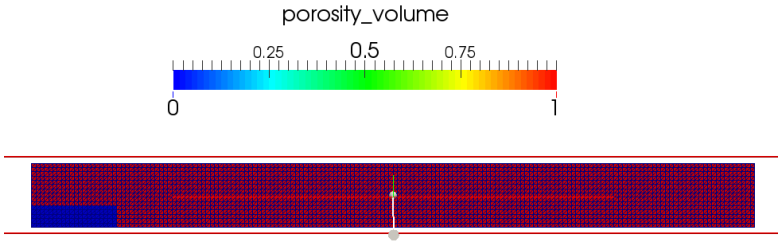

Figure 6 – Time mean velocity U along the centerline of the square cylinder.

Figure 7 and 8 show the vector velocity field as result of the simulation. It is possible to observe a recirculation zone after the step what is expected according to the literature and with what is observed in a real case.

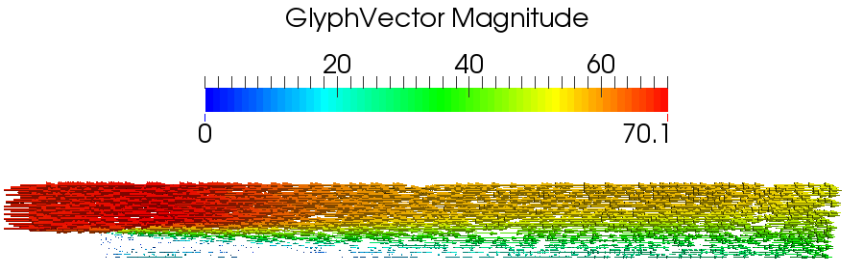

Figure 7 – Vector velocity field of the simulated turbulent flow over a step.

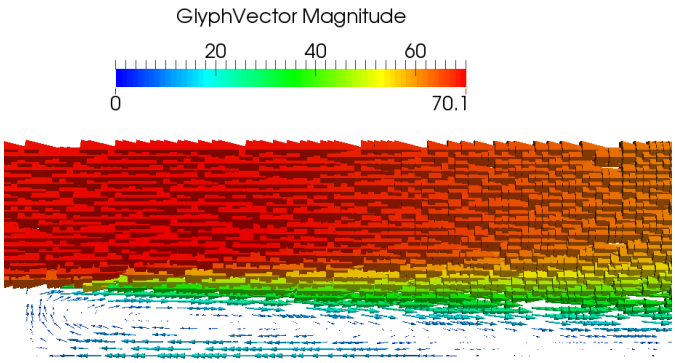

Figure 8 – Detailed vector velocity field of the simulated turbulent flow over a step.

The results of the simulation provided by the present solver (PFS) were compared with experimental data and other simulation that also uses the k-epsilon as turbulence model. Figures 9 and 10 show this comparison at four different distances from the step.

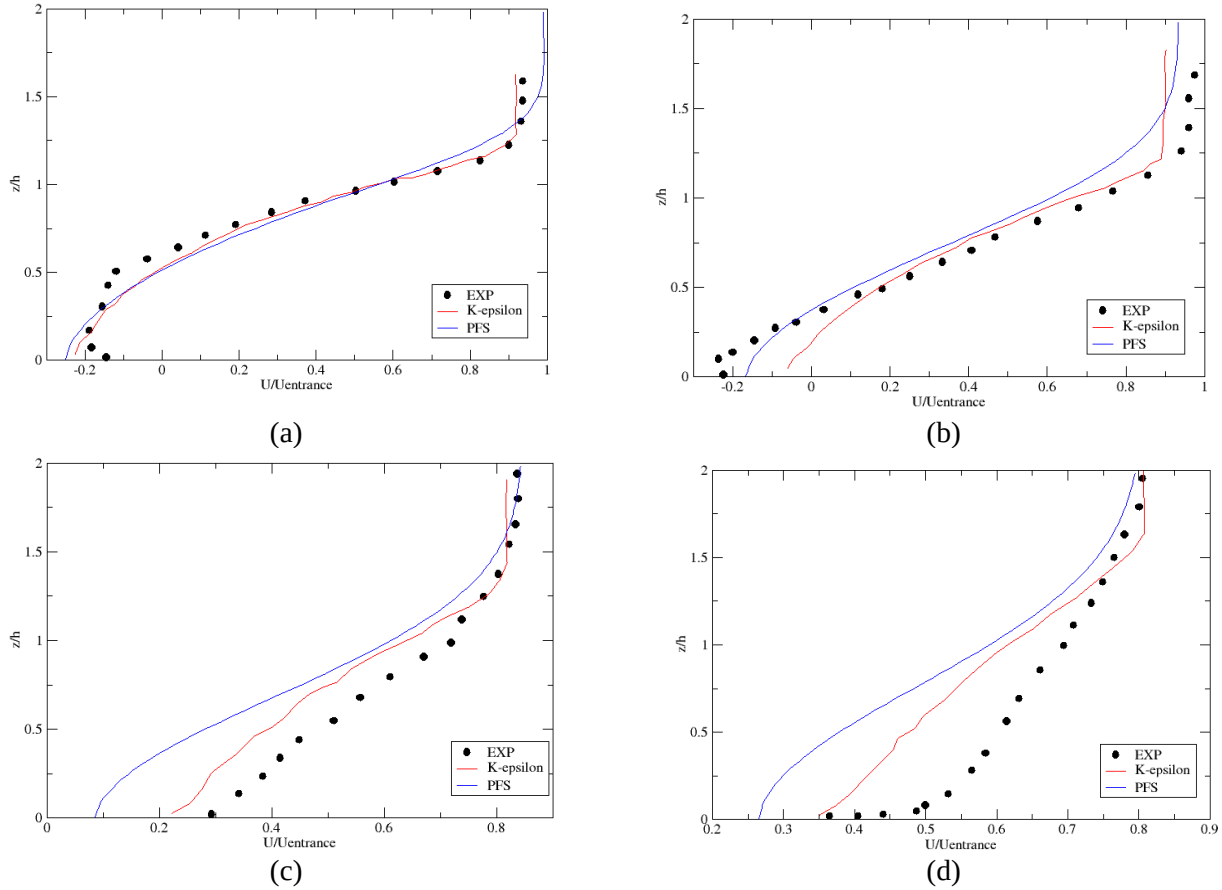

Figure 9 – Time mean velocity profile at different non-dimensional distances x/h (x represents the distance from the step and h the step height. (a) x/h=2.67; (b) x/h=5.33; (c) x/h=9.78; (d) x/h=16.

In Figure 9 it is possible to observe that the non-dimensional velocity profile provided by the present code is similar to the experimental data for a turbulent flow over a step. At the regions more closer from the step ((a) and (b)) the results provided by PFS are very similar to the experimental data. However, at the regions far from the step ((c) and (d) the results provided by PFS are slightly different from those given by experimental data. Such difference is also observed by other simulation that uses k-epsilon turbulence model, which indicates that it is possible a lack provided by the turbulence model.

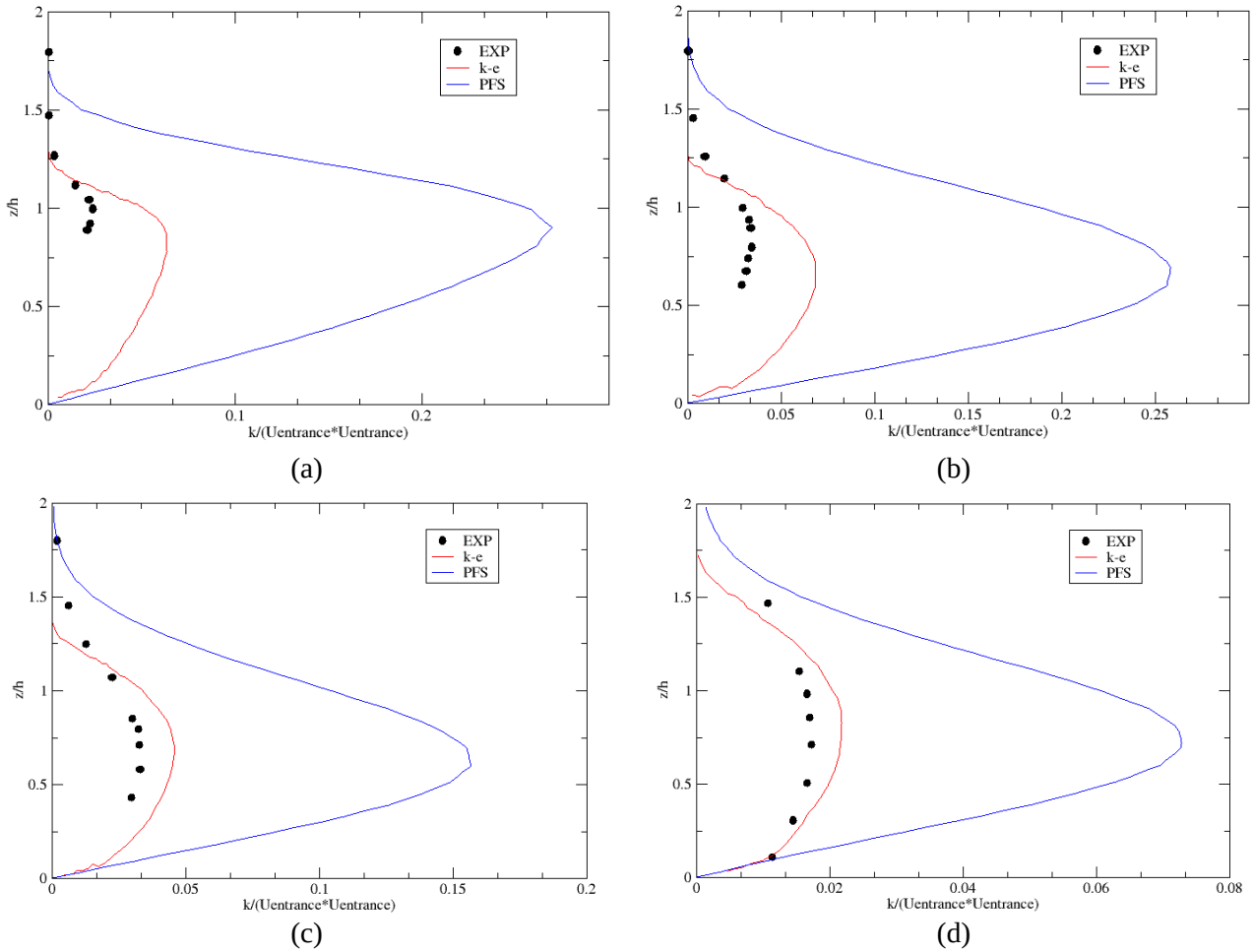

Figure 10 – Turbulence intensity at different non-dimensional distances x/H (x represents the distance from the step and H the step height. (a) x/H=2.67; (b) x/H=5.33; (c) x/H=9.78; (d) x/H=16.

In Figure 10 it is possible to verify that the turbulence intensity provided by PFS simulation have a similar profile to the experimental data and for a turbulent flow over a step. However, the values given by the present code overpredict the turbulence intensity. This observation is similar to that found previously for a turbulent flow over a rectangular cylinder.

Combustion Simulation

The previous tests have shown that the PFS tool is able to describe cold flow around buffed bodies. In a second step, preliminary tests have been conducted in order to evaluate the PFS code to describe the gas explosion phenomena. In this case, the flamelet concept state of the art have been used to model the combustion of a flammable gas.

At this stage a gas explosion in a combustion chamber was simulated by using the PFS code. The simulation was based on the work of SARLI et. al [11] who developed an experimental apparatus to analyze the gas explosion in a combustion chamber. The chamber comprises a rectangular box with 150 x 150 x 500 mm and contain three main obstacles (150 x 75 x 12 mm) that were positioned at 100 mm spacing within the chamber.

Figure 11shows a schematic representation of the explosion chamber used in this study. The experimental apparatus developed by SARLI et. al [11] are represented in the part (a). Part (b) presents the parametrized geometry used by PFS code.

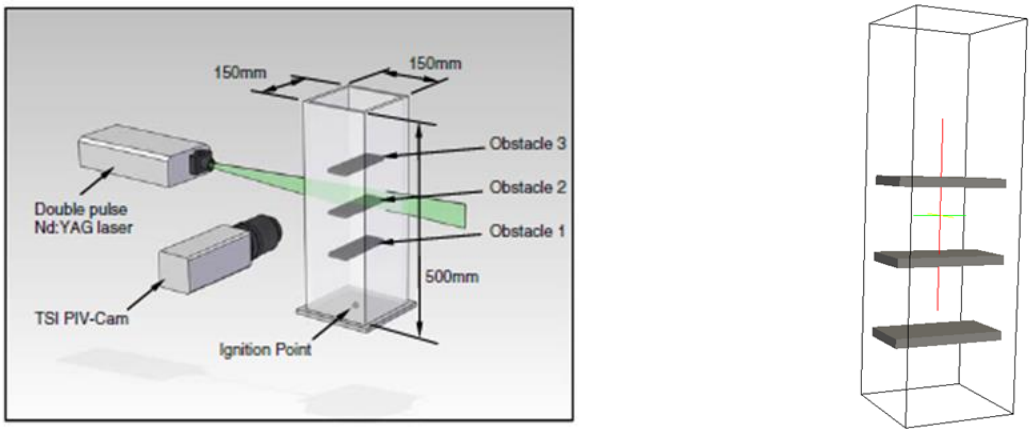

(a) (b)

Figure 11 – Schematic representation of a combustion chamber. (a) Experimental apparatus developed by SARLI at al [11] and (b) parametrized geometry provided by PFS code pre-processor.

Figure 12 shows the qualitative results given by the experimental analysis of a gas explosion in a combustion chamber (top of the figure) and the explosion simulation provided by the present code (bottom of the figure). In PFS results the blue zone represents the reactants and the red zone represents the products. The colorful region between the blue and red zones represents the flame front. It is possible to observe that the PFS code is able to predict the flame advanced at different times of the explosion. The qualitative results present a similar flame profile for the experimental data and the PFS simulation.

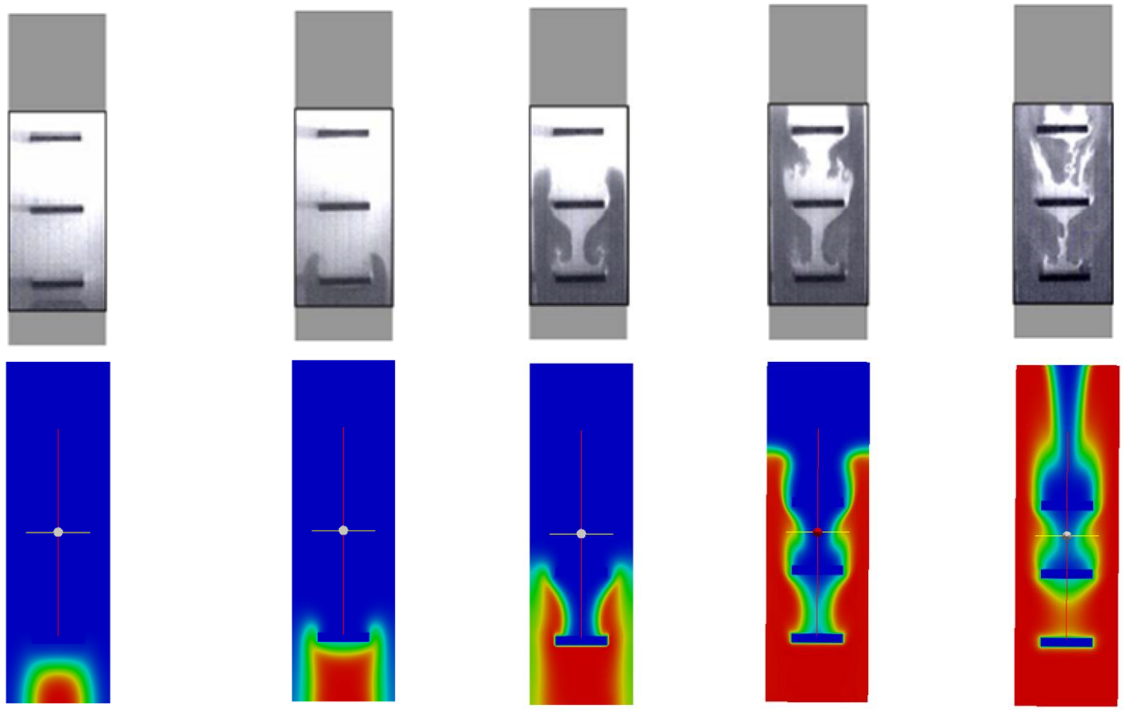

Figure 12– Time sequence of flame at the central plane of the combustion chamber. The PIV images provided by SARLI et al [11] are in the top of the figure while the PFS simulation results are in the bottom.

FINAL COMENTS

The Porosity Flow Solver was presented as an alternative tool to calculate flows. The results of the simulations of cold flows obtained by using the PFS code are in accordance with the literature and are also similar to the experimental data, especially for the velocity field and profile. When concerning the turbulence, the code overpredicts the turbulence intensity, so some adjustment have been performed in order

to make the code more realistic for the turbulence effects.

Preliminary results of the combustion simulation show that the code is also able to capture the flame behavior in a combustion chamber with obstacles.

REFERENCES

[1] R.S. CANT. "Modelling and simulation of accidental combustion in complex geometries". *In 5 International Seminar on Fire and Explosion Hazards*, (2007).

[2] R.S. CANT; W.N. DAWES; A.M SAVILL. "Advanced CFD and modeling of accidental explosion". *Annual Review in Fluid Mechanics*, 36, 97–119, (2004).

[3] J.K. WATTERSON; I.J. CONNELL; A.M. SAVILL; W.N. DAWES. "A solution adaptative mesh procedure for predicting confined explosion". *Journal of Numerical Methods in Fluids*, 26,235–247 (1988).

[4] C. FOTHERGILL; S. CHYNOWET; P. ROBERT; A. PACKWOOD. "Evaluation a CFD porous model for calculating ventilation in explosion hazard assessments". *Journal of Loss Prevention in the Process Industries*, 4, 6, 341–347 (2003).

[5] B.H. HJERTAGER; T. SOLBERG. "Computer modelling of gas explosion propagation in offshore modules". *Journal of Loss Prevention in the Process Industries*, 5, 3, 165–174, (1992).

[6] S.S.V. VIANNA; R.S. CANT. Modified porosity approach and laminar flamelet modelling for advanced simulation of accidental explosion. *Journal of Loss Prevention in the Process Industries*, 23, 3–14, (2010).

[7] V.D. MOREIRA; R.G.SANTOS; T.D.FERREIRA; S.S.V.VIANNA. "Towards Gilbert-Johnson-Keerthi Algorithm Distance for Fluid Flow Numerical Analysis". *23rd ABCM International Congress of Mechanical Engineering*. Rio de Janeiro, BR (2015).

[8] J.Y.YOO; H.C.CHOI; S.M.HAN. "Numerical analysis of turbulent flow over a backward-facing step using reynolds stress closure model". *KSM Journal*, 3, 31-37, (1989).

[9] D. A. LYN; S. EINAV; W. RODI; J.H. PARK. "A laser doppler velocimetry study of ensemble-averaged characteristic of the turbulent near wake of a square cylinder". *Journal of Fluid Mechanics*, 304, 285–319, (1995).

[10] W. RODI. "Comparison of LES and RANS calculations of the flow around bluff bodies". *Journal of Wind Engineering and Industrial Aerodynamics*. 69, 55-75, (1997).

[11] V.SARLI; A. BENEDETTO; G.RUSSO; S.JARVIS; E.J.LONG; G.K.HARGRAVE. "Large Eddy simulation and PIV measurements of unsteady premixed flames accelerated by obstacles". *Journal of Flow and Turbulence Combustion*. 83, 227-250, (2009).